A REDUCED COMPLEXITY DIGITAL MULTICARRIER DEMODULATOR FOR SATELLITE COMMUNICATION SYSTEMS

E Del Re, R Fantacci

Università di Firenze, Italy

INTRODUCTION

Satellite communications continue to undergo changes not only from advancing technology, but also from new service and regulatory activities. Therefore, advanced digital satellite communication systems using efficient modulation techniques and satellites with on-board processing capabilities are required. In particular, the on-board signal processing offers several advantages to satellite communication systems; an interesting feature is the separation of the uplinks and downlinks which permits their distinct and independent optimization. Regenerative satellites allow different modulation and multiple-access schemes to be employed in the uplinks and downlinks; for instance, uplink random access and downlink TDMA techniques can be envisaged (Ref. 1). Alternatively, for mobile communication services, the use of uplink FDMA techniques with the inherent low-cost earth stations, and downlink TDMA techniques that can fully exploit the satellite transponder output power without intermodulation, is a very interesting and attractive solution. However, the feasibility of this approach depends on efficient means to directly interface the two multiple access formats on-board the satellite. The on-board system implementation complexity (including the VLSI design) and power consumption are, of course, of primary concern. The on-board processing system receives an input FDMA signal and supplies an output to interface TDM links; therefore, it must accomplish the function of the separation of each individual radio channel and its demodulation. An appropriate name for the on-board processing system is the 'multicarrier demodulator' (MCD). Two main functions are implemented by a MCD: the demultiplexing (DEMUX) and the demodulation (DEMOD).

We focus here only on a digital implementation of the MCD because in perspective it offers several advantages such as flexibility, VLSI integrability, better efficiency. The operation of the DEMUX is to separate the individual input FDMA channels and to supply each of them to a demodulator input for the appropriate down-conversion to baseband. Therefore, in principle, its operation corresponds to a bank of band-pass filters followed by a down-converter. By digital means the down-conversion can be appropriately implemented by a decimation operation. On the other hand, the direct implementation of a bank of digital filters is not the most convenient solution. This paper describes an efficient approach to the digital implementation of the DEMUX, based on the analytic signal method (Ref. 2). This method fully exploits the properties of the analytic signal and employs the tools offered by the digital signal processing techniques to present a solution to the DEMUX that is modular, efficient, flexible, of relatively low complexity and suitable for VLSI integration. These characteristics can be achieved because the analytic signal approach directly leads to a per-channel and highly modular structure, and is highly flexible allowing to vary on demand the bandwidth assigned to each channel, simply by switching to a suitable new set of system parameters. Moreover, this method relaxes the requirements on the input analog anti-aliasing filter. Further, a certain degree of integration of the DEMUX and DEMOD functions is conceivable as will be shown later. A coherent demodulation is usually employed in satellite communications in order to achieve the required bit-error-rate (i.e. 10^{-6} to 10^{-9}) with an acceptable signal-to-noise ratio. The performance of a coherent demodulator depends rather critically on the design of the synchronization circuit employed to estimate the received carrier phase and bit synchronization reference from the received signal. The implementation structure of the MCD system considered herein is shown in Fig. 1. The digital architecture of the proposed MCD can be adapted to different digital modulation techniques; therefore, we focus here only on the application for QPSK signals, owing to the interest of this modulation scheme in satellite digital communications. The carrier recovery circuit has been implemented according to the non-linear estimation method proposed by Viterbi (Ref. 3). This method has been selected because it achieves a good estimate accuracy, is less sensitive to a finite arithmetic implementation and requires a short and definite acquisition time. Moreover, it can be applied to continuous as well as burst mode carriers and a certain degree of integration of the demultiplexer implemented according to the analytic signal method is conceivable (i.e. the separation of the in-phase and quadrature components of the received QPSK signal). The clock recovery circuit is assumed to be implemented according to a suitable clock recovery approach derived from that proposed by Gardner (Ref. 4). This clock recovery method has been selected because its estimation operations are independent of carrier phase and some degree of integration of demultiplexer and clock recovery functions is possible. An important feature of this clock recovery approach is that no explicit interpolation or decimation is required. Therefore, a lower overall MCD implementation complexity is achieved. In conclusion, the multicarrier demodulator described in this paper represents a complete solution for a processing system interfacing FDMA and TDM links. Its design has been carried out, in particular, aiming at its possible implementation by means of custom VLSI digital circuits.

DEMULTIPLEXER

The demultiplexing of a FDMA signal can be performed following two basic approaches: block methods and per-channel methods. We focus here on the analytic signal approach (Ref. 2) which is a per-channel method and has the specific feature to relax the filter specifications, thus achieving a lower implementation complexity with respect to other per-channel approaches. Further, the analytic signal approach directly leads to a per-channel and highly modular structure: this structure is directly matched to the per-channel implementation of the demodulators, and a certain degree of integration of the DEMUX and DEMOD functions is conceivable. The principle of operation of the analytic signal method has been reported in (Ref. 2). The structure of the DEMUX according to the analytic signal method is shown in Fig. 1 (Demultiplexer section) (Refs. 2,5,6). The FDMA input signal, after appropriate analog down-conversion of the received signal to a low frequency range, is sampled according

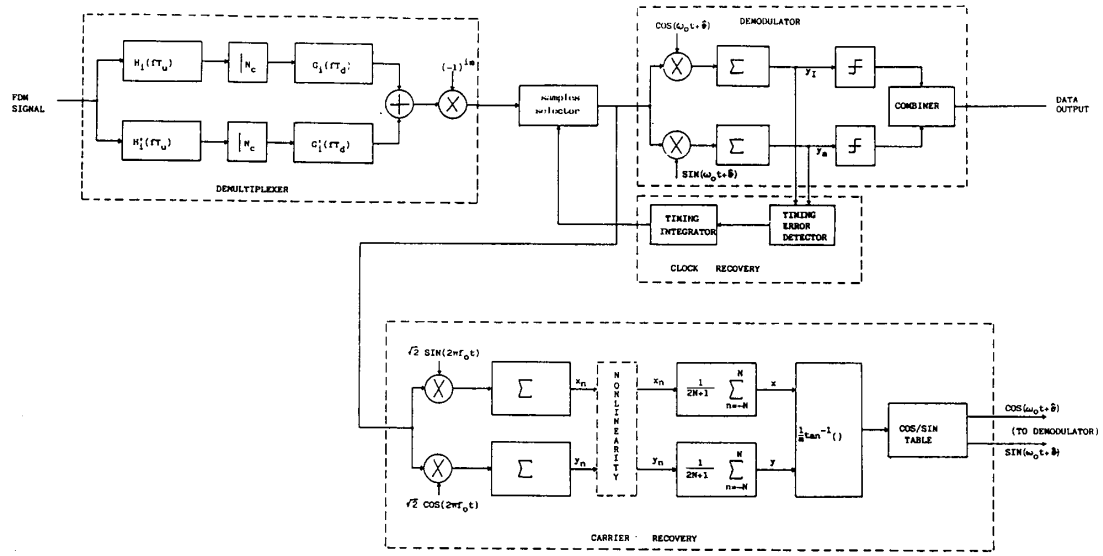

Fig. 1 - MCD structure.

to the sampling theorem (Ref. 7) at the high-rate frequency $f_u = 1/T_u$ and processed in order to obtain N_c baseband digital signals, each sampled at the low-rate frequency $f_d = 1/T_d = f_u/N_c$, N_c being the number of FDMA multiplexed channels. In Fig. 1, $H_i(fT_u)$, $H_i^!(fT_u)$ represent the conjugate symmetric and antisymmetric parts, respectively, of the high-rate complex bandpass filter $H_i(fT_u)$ which can be regarded as a frequency translated version of a lowpass prototype $H(fT_u)$ such that (Ref. 2):

$$H_i(fT_u)=H_i(fT_u)+jH_i^!(fT_u)=H[2\pi(f-iW-W/2)T_u] \qquad (1)$$

where W is the channel spacing. In the same figure, $G_i(fT_d)$ and $G_i^!(fT_d)$ represent the conjugate symmetric and antisymmetric parts, respectively, of the complex low-rate filter $G_i(fT_d)$ which can be defined as (Ref. 2):

$$G_i(fT_d)=G_i(fT_d)+jG_i^!(fT_d)=G\{[f-(-1)^i W/2]T_d\} \qquad (2)$$

$$i=1,2,\ldots N_c$$

Thus, each filter $G_i(fT_d)$ is related, according to eq. (2), to a lowpass prototype $G(fT_d)$. It can be noted from eq. (2) that the number of different filters $G_i(fT_d)$ is actually two: one for the odd channels and the other for the even channels. Taking into account eqs. (1) and (2), we have in the frequency domain (Refs. 2,5):

$$X_i(fT_d) = S[(fT_d + i/2)/N_c] \qquad (3)$$

according to the implementation structure shown in Fig. 1 (Demultiplexer section). The terms $S(fT_u)$ and $X_i(fT_d)$ in eq. 3 represent the spectrum of the input signal and the spectrum of the i-th output of the DEMUX, respectively. It must be noted that a decimation factor equal to the number N_c of multiplexed channels must be used and that only processing of real quantities is required. The overall number of multiplications and additions required per input channel and per second, denoted with M_{DEMUX} and A_{DEMUX}, respectively, in order to implement the demultiplexer according to the analytic signal approach, can be estimated as a function of the channel spacing W, the number of channels N_c and the filtering one-sided bandwidth B as (Ref. 6):

$$M_{DEMUX}=W^2[W(N_c+4)-2B(N_c+2)]/[(W-B)(W-2B)] \cdot \{-2[\text{Log } 5\ \delta_1\delta_2]/3\} \quad \text{(mults/sec.)} \qquad (4)$$

$$A_{DEMUX}=\{[-2\ \text{Log}(5\delta_1\delta_2)/3][N_c\ W/(W-B)+W/(2W-B)]-1\}4W \quad \text{(adds/sec.)}$$

where the terms δ_1 and δ_2 denote the overall acceptable in-band and out-of-band ripples, respectively, derived according to given system specifications; for example, a filter design procedure is reported in (Ref. 6). It results from eq. (4) that for specified values of B and N_c an optimum value for the channel spacing W_o can be found in order to achieve the lowest M_{DEMUX} and A_{DEMUX}. However, taking into account that for the subsequent demodulation operation an integer number of samples per symbol is convenient a suboptimum value of W closest to W_o is generally used which guarantees this condition. Thus, a suitable choice of the DEMUX output sampling frequency 2W turned out to be equal to 3 samples/symbol.

DEMODULATOR

In this section, the digital coherent demodulator for QPSK signals is considered. A digital coherent demodulator is comprised of three parts: i) the carrier recovery circuit; ii) the clock recovery circuit, and iii) the data decision circuit.

Carrier Phase Recovery

The carrier recovery circuit is assumed to be implemented by the non-linear estimation method proposed in (Ref. 3). Fig. 1 shows the general

structure of the phase estimator considered herein (carrier recovery section), where in the dotted box we suppose to insert the two dimensional (complex) non-linear functions:

$$x'_n + y'_n = \rho_n^2 \; e^{j4\Phi_n} \tag{5}$$

with $\rho_n = \sqrt{x_n^2 + y_n^2}$ $\Phi_n = \tan^{-1}(y_n/x_n)$.

In other words, for each symbol a rectangular-to-polar transformation is performed, multiplying phase Φ_n by 4, and squaring ρ_n. We avoid describing the non-linearity in this manner in Fig. 1, because in a practical implementation it becomes a read-only-memory, transforming a quantized two-dimensional vector into another such vector. Multiplying the phase by 4 along with the final operation of dividing the tan-1 function by 4, gives rise to a $\pi/2$ ambiguity in the phase estimates. A practical QPSK modulation system adjusts for this by coding the data transitions, rather than the data themselves (differential encoding), and performing the function of differential decoding at the receiver. Suppose we wish to estimate the phase at the midpoint of the estimation interval T_E, which encompasses (2N+1) QPSK symbols (each T long), the implementation complexity of the proposed carrier phase estimator can be derived as:

$$M_v = 3 \text{ R mults/sec.} \quad A_v = 2(N+1)R \text{ adds/sec.} \tag{6}$$

being R the transmission rate, and 3 samples per symbol have been assumed.

Clock Recovery and Data Decision

The main goal of the clock recovery circuit is to correctly select the set of three samples that belong to the same symbol. In other words, the timing error detector must partition the in-phase $y_I(\cdot)$ and quadrature $y_Q(\cdot)$ sample sequences into sets of three samples assumed to belong to a same symbol for the in-phase (I) and quadrature (Q) channel, respectively. By denoting with r the symbol number the timing error detector algorithm is of the following:

$$u(r) = [y_I^2(r) - y_I^2(r+1/3)] + [y_Q^2(r) - y_Q^2(r+1/3)] \tag{7}$$

The error sample u(r) is compared with a suitable threshold value V before activating the timing correction in order to reduce the influence of the intersymbol interference and the channel noise. The threshold value must be suitably determined in order to achieve a good tracking and acquisition performance. The timing correction is activated if :

$$\begin{aligned} &u(r) < -V \quad \text{and } y_I(r)y_I(r+1/3) > 0, \\ &\qquad y_Q(r)y_Q(r+1/3) > 0 \\ &u(r) > V \text{ and } y_I(r)y_I(r+1/3) < 0, \\ &\qquad y_Q(r)y_Q(r+1/3) < 0 \end{aligned} \tag{8}$$

In this case, the sequences $y_I(r)$ and $y_Q(r)$ are shifted back by one sample and a new partition of the received samples is considered. If the threshold V is suitably chosen, this algorithm achieves a good performance for both tracking and acquisition modes of operation; further, the error sample sequence u(.) is independent of carrier phase, so that timing lock can be achieved without depending upon power carrier phase lock. Once the timing error detection has selected the set of three samples which belong to the same symbol $\{y(r+1/3), i=0,1,2\}$ the data detection can be performed as follows:

i) the parameter $J = \sum_0^2 i \; y(r+1/3)$ is evaluated;

ii) $d_r = 1$ is assumed if $J > 0$, otherwise $d_r = -1$.

By assuming a correct partition of the sampled sequences $\{y_I(\cdot)\}$ and $\{y_Q(\cdot)\}$ an erroneous decision is due to the influence of the intersymbol interference and channel noise. The implementation complexity of the clock recovery circuit can be derived through eq. (7), taking into account the implementation complexity required to split the received QPSK signal into its in-phase and quadrature components, as:

$$M_c = 3 \text{ R mults/sec.} \quad A_c = 3 \text{ R adds/sec.} \tag{9}$$

Therefore, the overall implementation complexity of the coherent demodulator, including the decision circuit, is given by:

$$M_{DEMOD} = 6 \text{ R mults/sec/ch; } A_{DEMOD} = (2N+7)R \text{ adds/sec/ch} \tag{10}$$

SYSTEM DESIGN AND PERFORMANCE

In this section, the design of a MCD system is presented. The number of channels processed by the MCD influences the input sampling frequency and consequently the processing rate and the complexity of the first stage of the demultiplexer. In this paper, the number of channels N_C to be processed by the MCD has been selected taking into account the possibility of a variation of the transmission rate R in the range R to R/32 (with R = 4396 kb/sec.). Thus, the number of channels N_C should allow to vary the transmission rate with the lowest possible impact on the overall MCD structure. In particular, a feasible constraint is to require that the input A/D converter sampling frequency (clock) should be held constant at its maximum possible value. Starting from these considerations, as the design goal, we have selected $N_C = 3$ at R = 4396 kb/sec. In the following, a QPSK modulation technique with occupied signal bandwidth (i.e. filtering one-sided bandwidth B) equal to 0.3 R (KHz) at R = 4396 kb/sec., is assumed to be used for data transmission. The demultiplexer design is first presented. The high-rate and low-rate lowpass prototypes have been designed as a FIR linear phase filter by using the equiripple method (Ref. 8). The required filtering specifications are reported in Tab. 1 for $N_C = 3$. In the same table, the number of coefficients required for the high-rate lowpass prototype $H(fT_u)$ and low-rate lowpass prototype $G(fT_d)$ in order to satisfy the corresponding filtering specifications is also reported. It can be observed that the required pulse-shaping function (i.e. raised cosine with 40% roll-off factor) has been included in the low-rate lowpass prototype $G(fT_d)$. The demultiplexer finite precision design has been carried out in order to introduce at each demultiplexer output a degradation, with respect to an input signal-to-noise ratio SNRi equal to 7.6 dB, less than 0.2 dB. The derived finite arithmetic word-lenghts are reported in Tab. 2. In Fig. 2 and Tab. 4, the overall demultiplexer loss is reported for different values of E_b/N_o (at the DEMUX input). These degradations have been derived following the procedure outlined in (Ref. 6); they are due essentially to the effects of the required decimation process and of a finite precision implementation of the demultiplexer (Ref. 6). The coherent demodulator has been implemented according to the structure presented in Sect. 3. The demodulator implementation complexity can be derived through eq. (10) and the values obtained for $N_C = 3$ are reported in Tab. 3. In the same table, the overall MCD implementation complexity is also reported. In order to derive the degradations introduced by the coherent demodulator we have evaluated first the degradations

TABLE 1 - Filtering specifications for the analytic signal approach (N_c = 3).

	δ_1	δ_2	N.o of coefficients
High-rate filter H	$3.95 \cdot 10^{-2}$	$3.5 \cdot 10^{-2}$	9
Low-rate filter G	$3.95 \cdot 10^{-2}$	$3.5 \cdot 10^{-2}$	27

TABLE 2 - MCD Finite Arithmetic Wordlengths.

A/D Converter	DEMUX						DEMOD
	High-rate F			Low-rate F			
b_q	b_c	b_m	b_a	b_c	b_m	b_a	b_e
8	7	14	8	7	14	8	6

b_q = input signal quantization wordlength
b_c = filter coefficient wordlength
b_m = filter arithmetic wordlength
b_a = filter output wordlength
b_e = carrier and clock recovery wordlength

TABLE 3 - Implementation complexity of the MCD shown in Fig. 1 (N_c = 3).

DEMUX xR (mlt/s/ch)	DEMOD xR (mlt/s/ch)	OVERALL xR (mlt/s/ch)
47.25	6	53.25

TABLE 4 - MCD Loss Evaluation.

E_b/N_o (dB)	DEMUX LOSS (dB)	DEMOD LOSS (dB)	OVERALL LOSS (dB)
5	0.09	0.91	1
6	0.13	1.16	1.29
7	0.15	1.35	1.5
8	0.19	1.55	1.74

due to the phase jitter introduced by the carrier phase estimate and to a symbol timing offset introduced by the symbol timing estimate, by assuming them as two independent contributions (9). Further, in order to derive the overall degradation introduced by the coherent demodulator the effect of a finite precision implementation must also be taken into account. The achieved overall demodulator loss, including the degradation due to a finite precision implementation (Tab. 2) is reported in Fig. 2 and Tab. 4. In the same table and figure, respectively, the overall MCD degradation (demod loss plus demux loss) is also reported. In conclusion, the multicarrier demodulator described in this paper represents an attractive solution for processing systems interfacing directly FDMA and TDM links. It achieves a good performance with an acceptable on-board system implementation complexity. A further reduction in the overall implementation complexity can be achieved by integrating some demodulator and demultiplexer functions.

CONCLUSIONS

In this paper, the design of a completely digital multicarrier demodulator (MCD) for the application in advanced satellite communication systems has been presented. The proposed MCD has two parts:

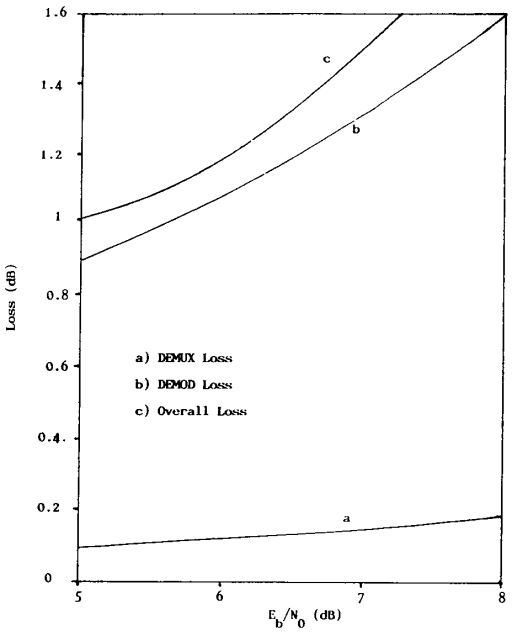

Fig. 2 - MCD loss as a function of E_b/N_o.

the demultiplexer (DEMUX) and the coherent demodulator (DEMOD). In particular, the DEMUX has been implemented according to the analytic signal approach leading to a per-channel structure that avoids any digital product modulator and any block processor. It has the specific feature to relax the filter specifications, thus achieving a lower implementation complexity with respect to other per-channel approaches. Further, the analytic signal approach is directly matched to the per-channel implementation of the demodulators;therefore, a certain degree of integration of the DEMUX and DEMOD functions can be obtained, thus lowering the overall system complexity. Another advantage of the analytic signal approach is its high flexibility: differently from other methods, in the case that some specific applications should benefit from the unequal channel bandwidth, the analytic signal structure could vary on demand the bandwidth assigned to each channel, simply by switching to a suitable new set of DEMUX parameters. The carrier recovery circuit has been assumed as implemented by a suitable carrier phase estimation approach which permits the achievement of a good estimate accuracy, is less sensitive to a finite arithmetic implementation and requires a short and definite acquisition time. The clock recovery circuit has been implemented according to a new estimation criterion which avoids any interpolation/decimation digital filter and permits to exploit the integration of the pulse-shaping function and separation of the in-phase and quadrature components in the low-rate stage of DEMUX. In conclusion, the digital MCD system described herein represents an appropriate solution for advanced digital communication systems interfacing FDMA and TDM links and, in particular, it has been carried out aiming at its possible implementation by custom or semicustom VLSI digital circuits.

REFERENCES

1. Benelli, G., Del Re, E., Fantacci, R., and

Mandelli, F., 1984, "Performance of Uplink Random-Access and Downlink TDMA Techniques for Packet Satellite Networks", Proc. IEEE, vol. 72, No. 11, 1583-1593.

2. Del Re, E., and Emiliani, P.L., "An Analytic Signal Approach to Transmultiplexers: Theory and Design", 1983, IEEE Trans. on Comm., vol. COM/30, No. 7, 1623-1628.
3. Viterbi, A.J., and Viterbi, A.M., "Non-Linear Estimator of PSK Modulated Carrier Phase with Application to Burst Digital Transmission, 1983, IEEE Trans. on Inf. Theory, vol. II/29, No. 4, 543-551.
4. Gardner, F.M., 1986, "A BPSK/QPSK Timing-Error Detector for Sampled Receivers", IEEE Trans. on Comm., vol. COM/34, No. 5, 423-429.
5. Del Re, E. et al., 1982, "Comparison of Non-FFT Methods of TDM-FDM Transmultiplexing", ALTA FREQ., No. 1, vol. LI, 9-21.
6. Estec Contract 6096/84/NLINGM(SC), Multicarrier Demodulator Design, Final Report, 1986.
7. Bellanger, M., 1984, "Digital Processing of Signals, Theory and Practice",John Wiley, London.
8. Programs for Digital Signal Processing, ASSP Dig. Sig. Process. Committee, Ed. IEEE Press, N.Y., 1979.
9. Matyas, R., 1978, "Effect of Noisy Phase Reference on Coherent Detection of FFSK Signals, IEEE Trans. on Comm., vol. COM/26, 807-815.